

DMD 27888

**Modulation of $\text{LogD}_{(7.4)}$ and pK_a to achieve the optimum balance of
blood clearance and volume of distribution for a series of
tetrahydropyran H_3 antagonists.**

Tanya Hay, Rhys Jones, Kevin Beaumont, Mark Kemp.

*Pfizer Global Research and Development, Sandwich, Kent, United Kingdom (TH, RJ,
KB, MK)*

DMD 27888

Modulation of $\text{LogD}_{(7.4)}$ and pK_a to achieve the optimum balance of blood clearance and volume of distribution for a series of tetrahydropyran H_3 antagonists describes how the modulation of lipophilicity and pK_a within a series can be used to optimise rat pharmacokinetic parameters to enable selection of an appropriate compound for further progression.

Author - Tanya Hay

Address - Pfizer Limited, Ramsgate Road, Sandwich, Kent, CT13 9NJ

e-mail address -tanya.hay@pfizer.com

telephone number - 01304642653

text pages - 16

words in abstract - 250

words in introduction - 248

words in discussion – 1536

figures – 5

tables - 4

references - 18

Non standard abbreviations used in the paper

ADME – Absorption, distribution, metabolism and excretion

API – Atmospheric pressure ionisation

AR – Allergic rhinitis

CNS – Central nervous system

H_3 – Histamine type 3 receptor

DMD 27888

LogP – The partition coefficient of a compound between octanol and water in its unionised form

LogD_(7.4) - The partition coefficient between octanol and buffer at pH 7.4

SAR – Structure activity relationship

THP – Tetrahydropyran

HLM – Human Liver Microsomes

RLM – Rat liver Microsomes

DMD 27888

Abstract

The relationship between the rat pharmacokinetics and the physicochemical parameters, $\text{LogD}_{(7.4)}$ and pK_a were studied for a series of tetrahydropyran (THP) compounds. Sixteen compounds ranging in $\text{LogD}_{(7.4)}$ 0.1 - 1.8 were administered intravenously to rats and the pharmacokinetic parameters determined from blood concentration time curves. Across the series, a weak correlation was observed between $\text{logD}_{(7.4)}$ and blood clearance, suggesting that $\text{logD}_{(7.4)}$ values lower than 0.5 were required to prevent clearance at hepatic blood flow. In terms of the volume of distribution, the compounds fell into three distinct sub series characterised by the number of basic centres and differences in ionisation of each basic centre at physiological pH. These were referred to as the monobasic, weak second base and strong second base sub-series. All compounds exhibited volumes of distribution greater than body water, as would be expected from their lipophilic and basic nature. For a given clogP the strong second base sub-series showed higher volumes of distribution than the weak second base sub-series, which in turn exhibited higher values than the monobasic sub-series. In addition, for the weak second base sub-series, volume of distribution could be tuned by modulating the pK_a of the second basic centre. This relationship was rationalized in respect to the interactions of the ionisable centres with phospholipid heads in the cell membrane and/or lysosomal trapping. Compounds in the weak second base sub-series showed optimal volumes of distribution and when combined with a $\text{logD}_{(7.4)}$ of 0.1, driving to moderate blood clearance, one compound showed the optimal pharmacokinetic profile.

DMD 27888

Introduction

The optimisation of ADME properties and prediction of human pharmacokinetics has become an important part of the early selection process in drug discovery. It is well known that the physicochemical properties of a molecule (lipophilicity, molecular weight, hydrogen bonding potential and pK_a) influence the pharmacokinetic profile of a molecule and the desirable ADME properties have been defined (van de Waterbeemd *et al.*, 2001a). In this paper, we describe how the modulation of lipophilicity and pK_a within a series of THP H₃ antagonists was used to optimise rat pharmacokinetic parameters and select an appropriate compound for further progression.

The objective of the H₃ antagonist programme was to rapidly accelerate a candidate compound to proof of concept studies in Allergic Rhinitis (AR). For the disease target in question, an orally administered compound with a once/twice daily dosing regimen was key to development. Neither CNS penetration nor CNS exclusion were requisites in the candidate as the site of action was peripheral.

In house medicinal chemistry resulted in the identification of a number of potent H₃ antagonists containing a tetrahydropyran (THP) core (Figures 1 and 2).

Figure 1. Core structure of the THP series

This present report details the optimisation of the pharmacokinetics within the THP series to identify a candidate for further progression. Key to the objectives was the identification of a compound with a predicted human half life in the range of 12-30 hours and an adequate oral bioavailability to allow a reasonably small dose (e.g. < 50 mg).

DMD 27888

Materials and methods

Materials. All H₃ antagonists were synthesised by the Discovery Chemistry department, Pfizer Global Research and Development. All other chemicals and reagents, unless stated otherwise, were purchased from Sigma-Aldrich Research (St.Louis, MO)

pK_a Determination. An accurate measurement of the ionisation constant values (pK_a) of the H₃ antagonists in a methanol-water binary mixture was performed by potentiometric titration. The potentiometric system consisted of a Sirius titrator GIpKa from Sirius Analytical Instruments Ltd (UK) with combined electrode; the GIpKa instrument was supplied with Sirius pK_a log P software for the calculation of pK_a. All measurements were carried out at constant temperature of 25 °C, constant ionic strength of 0.15 M KCl (adjusted to pH2 with 0.1 M HCl) and with a continuous flow of argon to prevent the absorption of CO₂ from the atmosphere. The solutions were then titrated with standardised KOH to pH12. The apparent ionization constants, *psKa*, were obtained at each co-solvent solution by a weighted non-linear least square procedure. The aqueous ionization constants, pK_{a 1} and pK_{a 2}, were obtained by Yasuda–Shedlovsky extrapolation of *psKa* values to 0% methanol (Gobry *et al.*, 2000)

LogD_(7.4) determination. The distribution coefficient of the H₃ antagonists between octan-1-ol and 0.1 M sodium phosphate buffer, pH 7.4 was determined by the shake flask methodology. This was completed in an automated manner with all liquid handling performed on a Hamilton Microlab star (8 probe) robot. 0.3 mg of compound was dissolved in 300 µL of octan-1-ol (pure, BDH, Poole, UK) and aliquoted in duplicate into a 96 well block. 300 µL of pre saturated buffer (2 L buffer pre saturated with 10 mL octan-1-ol) was added to the wells and the solution was

DMD 27888

vigorously mixed. After centrifugation the two phases were separated. 10 μL of a 1:200 dilution of the octan-1-ol layer and 10 μL of a 1:20 dilution of the buffer layer were directly injected on to the HPLC system described in full for the pharmacokinetic sample analysis. The peak areas were corrected for the dilution factors and the following calculation applied to determine the mean LogD value at pH 7.4.

$$\text{LogD}_{(7.4)} = \log^{10} \left(\frac{\text{peak area for octan-1-ol samples}}{\text{peak area for buffer sample}} \right)$$

***In vitro* metabolism studies in rat and human liver microsomes.** The standard incubation mixture contained 50 mM potassium phosphate (pH7.4), 5 mM MgCl_2 , 1mM NADP^+ , 5 mM isocitric acid and 1 unit/mL isocitrate dehydrogenase (NADPH was generated *in situ* by the isocitric acid isocitrate dehydrogenase system). Both rat and human incubations were carried out at 1 μM substrate concentration and 0.25 μM P450 concentration. Microsomes were purchased from BD Biosciences (Franklin Lakes, NJ) and were stored frozen in phosphate buffer at -80°C prior to use. Microsomal proteins were assayed by the method of Lowry and colleagues (Lowry *et al.*, 1951). The incubation mixture (without the NADP^+) was incubated at 37°C for 20 minutes. NADP^+ was then added to start the experiment. No co-factor and no drug controls were also prepared. Over a 60 minute period $9 \times 40 \mu\text{L}$ aliquots were removed from the incubation mix and added to 100 μL of ice cold acetonitrile. A 10 μL aliquot of 0.01 $\mu\text{g}/\text{mL}$ midazolam was added to each well for internal standardisation purposes. The precipitated proteins were pelleted by centrifugation for 30 minutes at 1507g and a 10 μL aliquot of the supernatant was injected onto a HPLC system. This consisted of an OPTI-LYNX cartridge C18 column (15x2.1 mm, Jay Tee Biosciences Ltd., Whitstable, Kent, UK) and an isocratic Jasco pump (Jasco,

DMD 27888

Tokyo, Japan) pumping at 2 mL/min. The eluting mobile phase was 90% methanol, 10% water, 2 mM ammonium acetate and 0.03% formic acid. Detection was by multiple reaction monitoring using a Sciex API3000 triple quadrupole mass spectrometer (Perkin Elmer, Boston, MA). The extent of microsomal binding was estimated using an in house *in silico* predictor. The intrinsic unbound clearance *in vitro* was calculated using the following equation adjusting the liver weight and concentration for the required species (Obach, 1997).

$$Cl_{int} = \frac{0.693 \times \text{liver weight}}{\text{In vitro } t_{1/2} \times \text{liver conc in incubation} \times cF_{u(\text{inc})}}$$

Blood binding determination. Control blood was collected in house, from male Sprague-Dawley rats and human volunteers, in potassium-EDTA tubes (Sarstedt, Inc. Newton, NC). Blood binding of the H₃ receptor antagonists was determined *in vitro* (n=6) by equilibrium dialysis (Spectrapor-1 dialysis membrane 6000-8000mol.wt cut-off; spectrum, Laguna Hills CA). 1 µg of compound was added to 1 mL rat/human blood and dialysed against isotonic Krebs-Ringer buffer (1 mL, pH_{7.4}) for 4 hours at 37 °C. 6 aliquots of 100 µL were taken from the blood and buffer sides at the end of the dialysis experiment. They were extracted and analysed by HPLC-MS analysis as described for the rat PK samples. Blood binding values were determined using the following equation:

$$\text{Blood binding (\%)} = 100 - \left(\frac{\text{buffer concentration}}{\text{blood concentration}} \right) \times 100$$

Single intravenous bolus dose rat pharmacokinetic dose preparation. Compound was accurately weighed and dissolved in 5% DMSO/saline to give a final concentration of 1 mg/mL. 1 mL/kg was dosed intravenously to each rat to give a

DMD 27888

final dose of 1 mg/kg. A dose check was performed at the end of the study and data only accepted if dose was within 20% of the initial concentration.

Animal experimentation. Male Sprague-Dawley rats (Charles River, Manston, UK) selected at a weight of approximately 250 g were used. Since rat pharmacokinetics were used in screening mode and only trends and gross differences between compounds were required, each compound was only dosed to n=1 rat. This increased speed, reduced compound requirements and most importantly, reduced the overall numbers of animals used for the study. Throughout the study animals were housed in stock boxes with access to food and water *ad libitum*. Single doses were administered as an intravenous bolus *via* the tail vein. Over a 24 hour period blood (approximately 175 μ L) was sampled into heparin coated tubes via a previously implanted *in situ* jugular vein cannula. The cannula was flushed with heparinised saline (10 units/mL) after each sample. All blood samples were diluted 1:1 with distilled water and stored at 4 °C prior to analysis. At all times these studies were carried out in accordance with the requirements of the United Kingdom national legislation and conducted using the appropriate guidelines.

Analysis of rat blood samples. Analyte was extracted from a 100 μ L aliquot of blood/water (1:1) following a liquid-liquid extraction technique. A volume of 10 μ L of a 1 μ g/mL solution of a structurally similar internal standard was added to each well. A volume of 1 mL of 0.1 M NaOH was added and the samples vortex mixed. This was followed by a further 2 mL of ethyl acetate. Each sample was vortex mixed for 30 seconds and centrifuged for 5 minutes at 1107g 4 °C to separate the organic and inorganic layer. The organic layer was removed using a pasteur pipette and transferred to a 96 well polypropylene block (Porvair sciences Ltd, UK). Samples were evaporated to dryness under a nitrogen flow at 37 °C and reconstituted in a

DMD 27888

volume of 300 μ L mobile phase A from which 180 μ L was injected onto the column. Chromatographic retention and separation was achieved on a Chromolith speed rod RP-18e 50 \times 4.6 mm column (OPTI-LYNX). The column was maintained at ambient temperature and the mobile phase flow rate was set at 3 mL/min with a 5:1 post column split using a Jasco pump (Jasco, Tokyo, Japan). The mobile phase composition was (A) 2 mM ammonium acetate in 90:10 methanol/water and 0.03% formic acid (B) 40% 2 mM acetonitrile both containing 10:90 methanol/water and 0.03% formic acid 2% using a ballistic gradient. Under these conditions all compounds were eluted at 2.5 ± 0.5 minutes. The total run time injection to injection was 3.5 minutes. A Sciex API 4000 with a Turboionspray interface (Perkin Elmer, Boston, MA) was used as the detector. Electrospray ionisation using positive ion multiple reaction monitoring (MRM) was the detection mode. Chromatograms were integrated using Analyst 1.4. software which was configured to automatically calculate and annotate the peak areas of both analyte and internal standard. Calibration curves were constructed using peak area ratios of the calibration samples and applying a 1/response (1/Y) weighted linear regression analysis. Analyte concentrations were calculated from the ratio of the analyte peak area to the internal standard peak area, interpolated from the calibration line.

Data analysis The following pharmacokinetic parameters were determined from individual animal data.

1. **Half life ($t_{1/2}$)** was calculated from the relationship $(0.693 \times Vd)/Cl$
2. **Area under the concentration versus time curve (AUC)** calculated to the last time point using the linear trapezoidal rule and extrapolated to infinite time using the terminal elimination rate constant. Extrapolated AUC was <20% of 0 hours to last time point AUC.

DMD 27888

3. **Clearance (Cl)** was calculated by the relationship dose/AUC.
4. **Volume of distribution (Vd)** was calculated by the relationship Cl/K_{el} .
5. **Unbound volume of distribution (Vdu)** was calculated by dividing the total Vd obtained from the intravenous pharmacokinetics by the free fraction of compound in the rat blood (van de Waterbeemd *et al.*, 2001b)
6. **Unbound clearance (Clu)** was calculated by dividing the total Cl obtained from the intravenous pharmacokinetics by the free fraction of compound in the rat blood (van de Waterbeemd *et al.*, 2001b)

DMD 27888

Results

Physicochemical properties of the H₃ antagonists

The structure and physicochemical properties of a subset of compounds from the THP series are shown in Table 1 and Figure 2. Many of the physicochemical properties are determined from computational models validated using algorithms and descriptors generated in house (clogP, HBA, HBD). Compounds are basic ($pK_a > 6.5$) and moderately lipophilic (clogP 1.8-3.9 and $\log D_{7.4}$ 0.1 to 1.2) in nature containing either one or two basic centres. The molecular mass is less than 500 (318 – 448) and they have a range of hydrogen bond donor and acceptor counts.

Table 1. Physicochemical properties of H₃ antagonists

Figure 2. Structure of compounds in the THP series

In vitro Cytochrome P450 metabolism of the H₃ antagonists

The majority of the compounds assessed *in vitro*, exhibited intrinsic clearance values of $<7 \mu\text{L}/\text{min}/\text{mg}$ protein in rat and human liver microsomes (Table 2) and low intrinsic clearance ($< 8 \mu\text{l}/\text{min}/10^6$ cells) in hepatocytes (data not shown). Where metabolism was observed in rat liver microsomes, the data were corrected for microsomal binding using an *in silico* predictor to determine the free fraction in the incubation mix (Hallifax and Houston, 2006).

Table 2. *In vitro* P450 metabolism of H₃ antagonists

DMD 27888

Blood Binding of the H₃ antagonists

The H₃ antagonists exhibited moderate blood binding values which translated to a free fraction in the blood ranging from 0.13 – 0.64. Individual values were used to calculate the rat Cl_u values listed in table 3.

Intravenous pharmacokinetics of the H₃ antagonists in the rat

The rat pharmacokinetic data of compounds in the THP series are summarised in table 3. A limitation of this study was the screening nature of the rat pharmacokinetic studies, using one animal per time point. As discussed in the methods section, this was felt appropriate since only trends and gross differences between compounds were to be considered.

In keeping with the basic nature of the series, all compounds exhibited volumes of distribution greater than that of body water. Following an intravenous bolus dose of 1mg/kg, compounds 1-3 containing one basic centre at R1, displayed blood clearance values in excess of liver blood flow (Boxenbaum, 1980). The half life of these compounds was ≤1 hour. Compounds 4 – 11 contain a second basic centre at R2 that is partially ionised at physiological pH. The clearance of these compounds tended towards hepatic blood flow and the volumes of distribution ranged from 12-62 L/kg. Together these factors combined to give half lives in the rat of 3-18 hours. Compounds 12 to 16 contain two strongly basic centres, both of which are essentially fully ionised at physiological pH. The volumes of distribution ranged from 30 – 99 L/kg, and the blood clearance values ranged from 5 to 32 mL/min/kg. The half life values of these compounds ranged between 22 and 60 hours.

Table 3 Rat intravenous pharmacokinetic properties of compounds in the THP series

DMD 27888

Discussion

The objective of the H₃ antagonist programme was to rapidly accelerate a first in class compound to proof of concept studies for the treatment of AR. Key to progression was the identification of a compound with a human half life sufficiently long to minimise the variability in drug concentrations, whilst providing exposure suitable for efficacy. The medicinal chemistry team identified the THP series in which H₃ potency and selectivity at the target were observed, in addition to chemical tractability. All compounds were “rule of five” compliant (Lipinski, 2000; Leeson and Springthorpe, 2007) and therefore adequate oral absorption was expected.

In general, the compounds were slowly metabolized by *in vitro* systems using rat and human liver microsomes (Table 2). These *in vitro* systems could not be used to select among compounds and the compounds were therefore progressed to rat pharmacokinetic studies. In these studies, the compounds exhibited blood clearance values from 5 to 240 mL/min/kg. The lack of *in vitro/in vivo* correlation suggested that hepatic metabolism was not responsible for the observed *in vivo* clearance. The absence of unchanged compound in urine and bile (Pfizer in house data) suggested that renal and biliary elimination were also not significant clearance pathways. Thus, the clearance pathway for this series of compounds remained unknown. It was rationalised that selection of compounds for further progression could be achieved on the basis of scaling rat clearance to human using single species (assuming similar clearance pathways) and estimating human Vd by accounting for protein binding differences between rat and human (Hosea *et al.*, 2009). The predicted human half life was then calculated using $t_{1/2} = (0.693 * Vd) / Cl$. Examination of blood clearances in rat across the whole series suggested a weak correlation with $\log D_{(7.4)}$ (Figure 3).

Figure 3 Correlation between rat blood clearance and measured $\log D_{(7.4)}$

DMD 27888

In general, compounds at the higher end of the $\log D_{(7.4)}$ range (ie >1) tended towards high clearance relative to hepatic blood flow. At the lower $\log D_{(7.4)}$ range (<0.5), the clearance values were low to moderate with respect to hepatic blood flow. This empirical observation suggested that for this series, to be in an appropriate blood clearance range, a compound should possess a $\log D_{(7.4)}$ of less than 0.5.

All of the H_3 antagonist compounds studied exhibited volumes of distribution significantly above body water (Table 3). This was expected since all compounds within the series contain at least one strongly basic centre (Rodgers *et al.*, 2005) and are lipophilic bases (van de waterbeemd *et al.*, 2001a).

Examination of the compound series with respect to ionization potential yielded some interesting observations. All of the compounds contain one strongly basic centre ($pK_a >8.9$). However, a number of compounds also contain a second basic centre, ranging from weakly basic (pK_a values 6.5 to 7.6) to strongly basic ($pK_a >9.0$). Thus, there were 3 potential sub-series: monobasic, weak second base and strong second base. The monobasic sub-series (compounds 1 to 3) exhibited short elimination phase half life values due to the combination of greater than hepatic blood flow clearance and moderate volumes of distribution. In contrast, the elimination phase half life values of the dibasic series were considered too long (22 to 60h) in the rat to be suitable for once daily dosing in human. These values remained long despite attempts to modulate Log P (to increase clearance of compounds 12 to 16) since clearance and volume of distribution changed similarly with log P.

In an attempt to identify a compound with ideal pharmacokinetic properties (low clearance, moderate volume of distribution and moderate half life) a strategy to maintain $\log D_{7.4}$ below 0.5 and modulate volume of distribution by altering the basicity of the second based centre was used. Compounds 4 to 10 were synthesised

DMD 27888

with a second basic centre ranging in pK_a from 6.5 to 7.6. A positive correlation was observed between unbound volume of distribution and the pK_a of the weak second basic centre (figure 4). As a result a range of elimination half lives were observed (3 to 18h). This suggests that the volume of distribution of the weak second base sub-series can be tuned by modulating the pK_a of the second basic centre. There are two potential explanations for this relationship (figure 5).

Figure 4. Correlation between the pK_a of the second basic centre and the V_{du} for compounds with a weak second basic centre.

Firstly, basic molecules are believed to express their tissue distribution through binding to the phospholipids that make up cell membranes (van de Waterbeemd *et al.*, 2001a).

The membrane partitioning theory is based on the slightly acidic extra-cellular environment driven by the negative charges on the phospholipid head groups of the cell membrane. A monobasic compound with a pK_a of 9.4 will be 99.9% ionised under these conditions (pH 6.4 used for illustration purposes). Tissue distribution for this base will be a combination of the electrostatic interaction of the positive charge with the negatively charged phospholipid heads, combined with lipophilic interactions with the triglyceride tails. The introduction of a second basic centre introduces a second positive charge that potentially adds a further electrostatic interaction. The pK_a of the second basic centre will determine the extent of ionisation at that centre and therefore the extent of the second interaction. For example, under these conditions a second pK_a of 6.4 will be 50% ionised, a pK_a of 7.4 will be 90% ionised and a pK_a of 9.4 will be 99.9% ionised. If the degree of secondary interaction drives further tissue

DMD 27888

distribution, then it would be expected that the volume of distribution values would increase with increasing second pK_a .

Figure 5. Proposed mechanisms for the effects of modulating the pK_a of the second basic centre.

The second potential mechanism to explain the observed volume of distribution relationship of these compounds is lysosomal trapping (Daniel and Wojcikowski, de Duve, Chanteux 1997). On entering into the lysosomal compartments within the cell, the pH changes to become a more acidic environment. Thus, the bases will be pushed towards a greater degree of ionisation. Since only unionised molecules can partition across membranes, the rate of passive return to the blood will depend upon the degree of ionization of the molecule, which in turn depends on the pK_a relative to the pH within the lysosome. The monobasic compound with a pK_a of 9.4 will be 99.99% ionised at this pH, with 0.01% present in the unionised form. The rate of partition of the unionised form back into the blood will determine the volume of distribution. The introduction of a second weak base (of pK_a 6.4 or 7.4) will lower the amount of unionised molecules (i.e. only 1 or 10% of the 0.01% will be unionised) and should reduce the rate at which the compound can permeate back into the blood, and thus increase the volume of distribution.

The contribution that lysosomal trapping makes to the distribution of molecules has been studied using an *in situ* perfusion of the isolated rat liver (Siebert et al, 2003). These authors suggested that the hepatic distribution of atenolol (Log Papp 0.14) was mainly determined by lysosomal trapping, whereas for the more lipophilic propranolol (Log Papp 3.1) distribution was equally determined by lysosomal trapping and binding to membranes. Since the H_3 antagonists studied in this investigation exhibit clog P values above 1.8, membrane binding is likely to be a major contributor to their

DMD 27888

distributional behaviour. This was further underlined by a series of tissue affinity experiments (data not shown).

In summary, the H₃ antagonist sub-series explored enabled the rational design of a compound with optimum pharmacokinetics. The monobasic series could be ruled out on the basis of the observed liver blood flow clearance and moderate volumes of distribution, leading to short elimination phase half life values in the rat and poor oral bioavailability. The strong second base series was discounted on the basis of rat pharmacokinetic parameters. These compounds tended towards moderate blood clearance and exhibited large volumes of distribution. Consequently, the terminal elimination phase half life values were long (greater than 22 hours). Extrapolation of the human pharmacokinetics of these compounds suggested the potential for acceptable oral bioavailability, but with extremely long terminal elimination phase half life values (>100hr). Pharmacokinetic profiles such as this are not ideal for compound development since such compounds take many doses to reach steady-state. In addition they add a level of complexity to clinical trials in terms of wash out reducing the feasibility of crossover designs, and are not easily withdrawn if a serious side-effect becomes apparent.

Table 4. The rational design towards the ideal H₃ PK profile in rat

For the third series with one strong and one weakly basic centre, the volumes of distribution were intermediate between the monobasic and the strong second base sub-series. In this series, the acceptable clearance with respect to hepatic blood flow could be achieved by maintaining logD_(7.4) below 0.5, while the volume of distribution could be tuned through modulation of the pK_a of the second basic centre. Combined with a moderate volume of distribution, the predicted terminal elimination phase half

DMD 27888

life would be acceptable for once or twice daily administration. The characteristics across the 3 series explored are best exemplified by compounds 1, 12 and 11 (Table 4)

Compound 11 was selected for further progression.

DMD 27888

Acknowledgments

We would like to acknowledge Patrick Bernardelli for his input into the design and synthesis of a number of the early compounds within the THP series.

DMD 27888

References

- Boxenbaum H (1980). Interspecies variation in liver weight, hepatic blood flow and antipyrine intrinsic clearance: extrapolation of data to benzodiazapines and phenytoin. *J Pharmacokinet Biopharm* **8**:165-176.
- Chanteux H, Paternotte I, Mingeot L.P, Brasseur R, Sonveaux E and Tulkens PM (2003) Cell handling, membrane-binding properties, and membrane-penetration modeling approaches of pivampicillin and phthalimidomethylampicillin, two basic esters of ampicillin, in comparison with chloroquine and azithromycin. *Pharmaceutical research* **20**:624-631.
- Daniel WA and Wojcikowski J (1997) Contribution of lysosomal trapping to the total tissue uptake of psychotropic drugs. *Pharmacology and toxicology* **80**:62-68.
- de Duve C, de Barsey T, Poole B, Trouet A, Tulkens P, Van Hoof F (1974) Lysosomotropic agents. *Biochemical Pharmacology* **23**: 2495-2531
- Gobry V, Bouchard G, Carrupt PA, Testa B and Girault HH (2000) Physicochemical characterization of sildenafil: Ionization, lipophilicity behavior, and ionic-partition diagram studied by two-phase titration and electrochemistry. *Helvetica Chimica Acta* **83**:1465-1476.
- Hallifax D and Houston JB (2006) Binding of drugs to hepatic microsomes: comment and assessment of current prediction methodology with recommendation for improvement. *Drug metabolism and disposition: the biological fate of chemicals* **34**:724-726.
- Hosea NA (2009) Prediction of human pharmacokinetics from preclinical information: Comparative accuracy of quantitative prediction approaches. *J Clin Pharmacol* **49**: 513-533.

DMD 27888

- Leeson PD and Springthorpe B (2007) The influence of drug-like concepts on decision-making in medicinal chemistry. *Nature Reviews Drug Discovery* **6**:881-890.
- Lipinski CA (2000) Drug-like properties and the causes of poor solubility and poor permeability. *Journal of pharmacological and toxicological methods* **44**:235-249.
- Lowry OH, Rosenbrough NJ, Farr AL, Randall RJ (1951) Protein measurement with the Folin phenol reagent. *J. Biol Chem* **193**:265-275.
- Nightingale CH (1997) Pharmacokinetics and pharmacodynamics of newer macrolides. *The Pediatric infectious disease journal* **16**:438-443.
- Obach RS (1997) Nonspecific binding to microsomes: impact on scale-up of in vitro intrinsic clearance to hepatic clearance as assessed through examination of warfarin, imipramine, and propranolol. *Drug metabolism and disposition: the biological fate of chemicals* **25**:1359-1369.
- Rodgers T, Leahy D and Rowland M (2005) Physiologically based pharmacokinetic modeling 1: predicting the tissue distribution of moderate-to-strong bases. *Journal of pharmaceutical sciences* **94**:1259-1276.
- Shepard RM, Falkner FC and Corporate author P Pharmacokinetics of Azithromycin in Rats and Dogs. *J-Antimicrob-Chemother* **25**:49-60.
- Siebert GA (2003) Ion trapping, Microsomal binding and unbound drug distribution in hepatic retention of basic drugs. *Journal of pharmacological and experimental therapeutics* **308**:228-235.
- Smith D (2001). Absorption and distribution as factors in drug design. Medicinal chemistry into the millennium (ISBN 0-85404-769-7) 332-344

DMD 27888

van de Waterbeemd H, Smith DA, Beaumont K and Walker DK (2001a) Property-based design: optimization of drug absorption and pharmacokinetics. *Journal of medicinal chemistry* **44**:1313-1333.

van de Waterbeemd H, Smith DA and Jones BC (2001b) Lipophilicity in PK design: methyl, ethyl, futile. *Journal of computer-aided molecular design* **15**:273-286.

DMD 27888

Legends for Figures

Figure 1. Core structure of the THP series

Figure 2. Structure of compounds in the THP series

Figure 3 Correlation between rat blood clearance and measured $\log D_{(7.4)}$

Figure 4. Correlation between the pK_a of the second basic centre and the V_{du} for compounds with a weak second basic centre.

Figure 5. Proposed mechanisms for the effects of modulating the pK_a of the second basic centre.

DMD 27888

Tables

Table 1. Physicochemical properties of H₃ antagonists

Compound	Molecular mass	clogP	log D _(7.4)	pKaR1	pKaR2	HBA	HBD
1	340	1.8	1.1	9.2	n/a	3	0
2	400	3.9	1.5	10.4	n/a	4	0
3	400	1.8	1.0	8.9	n/a	3	1
4	395	3.8	1.0	10.4	6.5	3	1
5	396	3.7	1.1	10.4	6.6	3	0
6	388	2.7	0.9	9.3	6.7	3	0
7	388	2.8	0.8	10.4	6.7	3	0
8	409	3.7	1.1	10.0	6.9	3	1
9	395	3.8	1.1	10.4	6.9	3	1
10	448	4.9	1.2	10.4	7.6	3	1
11	410	3	0.1	10.4	6.6	4	1
12	360	2.6	0.1	10.4	9.0	2	0
13	318	2.1	0.2	10.0	10.0	2	2
14	390	3.2	0.2	10.0	9.6	3	0
15	386	4.1	0.3	10.4	9.3	2	0
16	372	3.5	0.4	9.3	9.0	2	0

HBD, Hydrogen bond donor, HBA, Hydrogen bond acceptor

Table 2. In vitro P450 metabolism of H₃ antagonists

Compound	Calculated <i>f_u(inc)</i>	HLM Clint, _{un}	RLM Clint, _{un}
		<i>μL/min/mg protein</i>	
1	0.58	<7	27
2	0.44	<7	19
3	0.89	<7	20
4	n/a	<7	<7
5	n/a	<7	<7
6	n/a	<7	<7
7	n/a	<7	<7
8	n/a	<7	<7
9	n/a	<7	<7
10	n/a	<7	<7
11	n/a	<7	<7
12	n/a	<7	<7
13	n/a	<7	<7
14	n/a	<7	<7
15	n/a	<7	<7
16	n/a	<7	<7

HLM, Human liver micorosomes, RLM, Rat liver micorosomes

Clint,_{un}, unbound intrinsic clearance

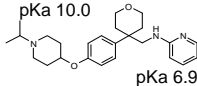
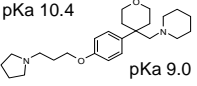
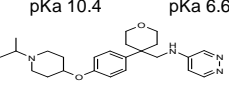
DMD 27888

Table 3 Rat intravenous pharmacokinetic properties of compounds in the THP series

Series	Compound	logD _(7.4)	pKa1	pKa2	Cl mL/min/kg	Cl _u mL/min/kg	Vd L/kg	Vdu L/kg	T1/2 hr
Monobasic	1	1.1	9.2	n/a	240	>511	6.5	14	0.3
	2	1.5	10.4	n/a	117	>418	6.0	21	0.6
	3	1.0	8.9	n/a	92	>144	7.7	12	1.0
Weakly dibasic	4	1.0	10.4	6.5	93	>245	27	71	3.0
	5	1.1	10.4	6.6	78	>181	19	44	2.8
	6	0.9	9.3	6.7	122	>244	36	72	3.4
	7	0.8	10.4	6.7	134	>268	39	78	3.3
	8	1.1	10.0	6.9	128	>492	41	157	3.7
	9	1.1	10.4	6.9	41	171	32	97	9.0
	10	1.2	10.4	7.6	40	121	62	258	18
	11	0.1	10.4	6.6	30	150	12	60	4.6
Strongly dibasic	12	0.1	10.4	9.0	18	86	94	455	60
	13	0.2	10.0	10.0	5	15	30	37	31
	14	0.2	10.0	9.6	32	178	60	339	22
	15	0.3	10.4	9.3	24	186	99	788	48
	16	0.4	9.3	9.0	10	59	33	197	39

DMD 27888

Table 4. The rational design towards the ideal H₃ PK profile in rat

	 <p>pKa 10.0 pKa 6.9 Monobasic</p>	 <p>pKa 10.4 pKa 9.0 Strongly Dibasic</p>	 <p>pKa 10.4 pKa 6.6 Weakly Dibasic</p>
	Compound 1	Compound 12	Compound 11
logD ^(7.4)	1.1	0.1	0.1
clog P	1.8	2.6	3.0
Cl mL/min/kg	240	18	30
Clu mL/min/kg	>511	86	150
Vd L/kg	6.5	94	12
Vdu L/kg	14	455	60
Half life h	0.3	60	5
Predicted human half life (h)	<2.0	250	18

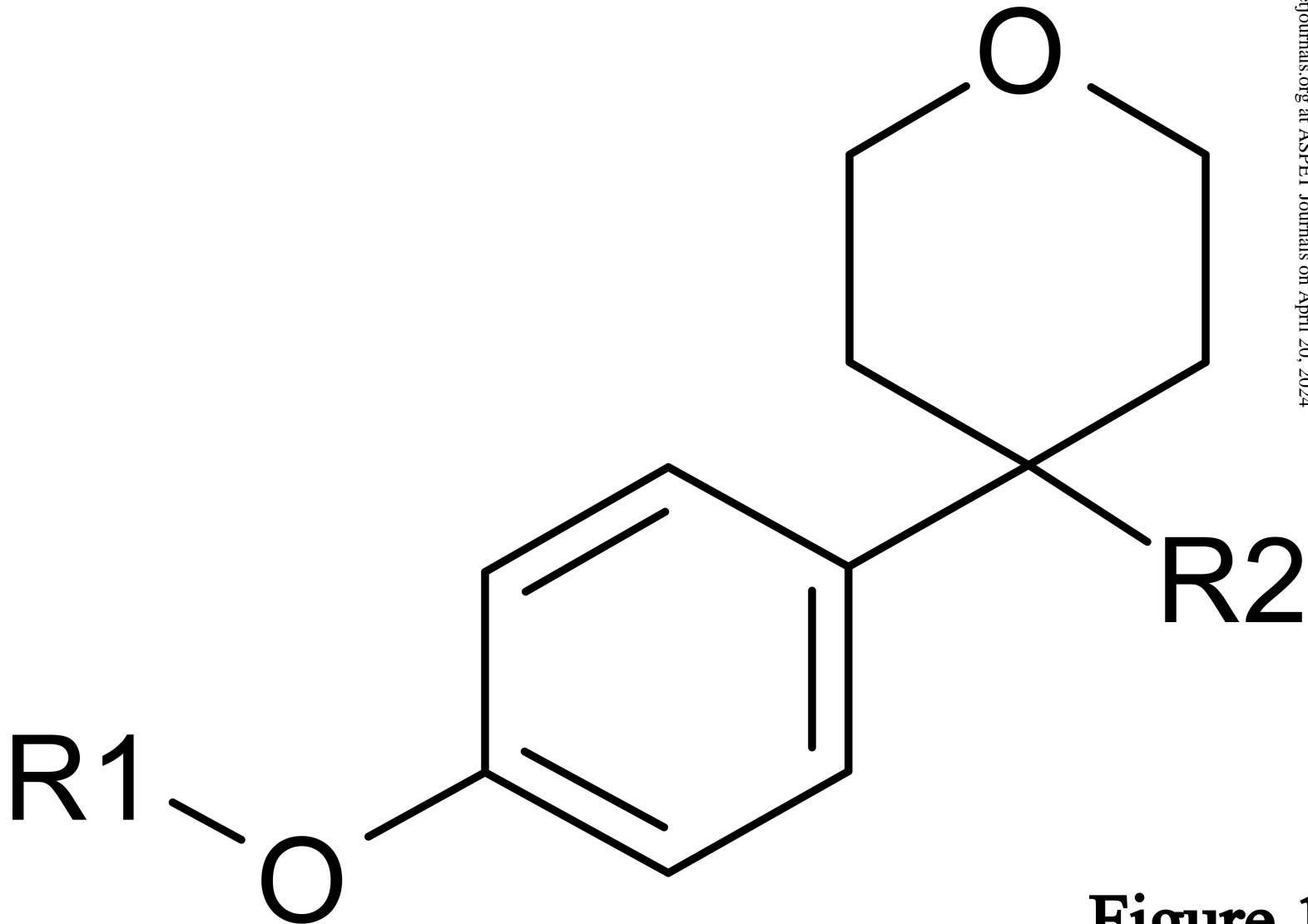
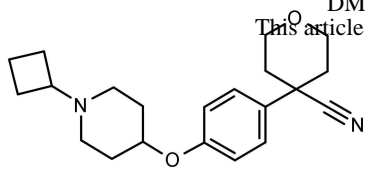
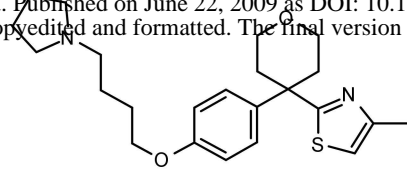


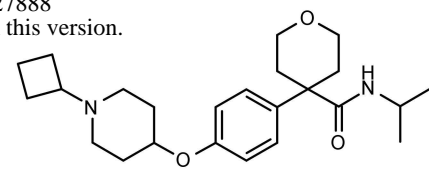
Figure 1



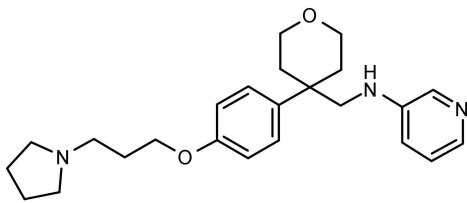
1



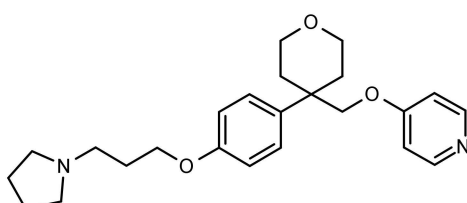
2



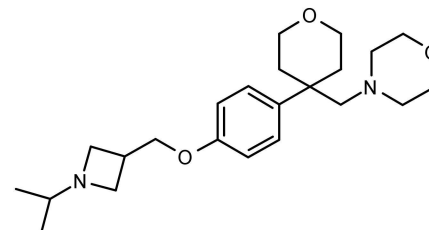
3



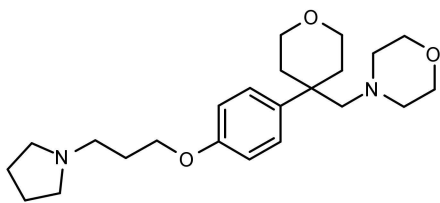
4



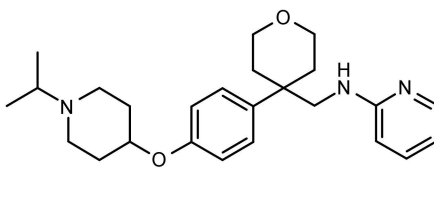
5



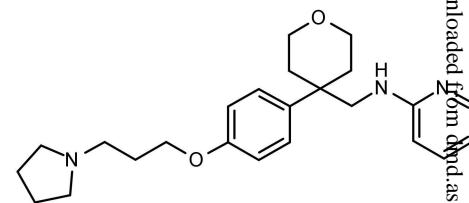
6



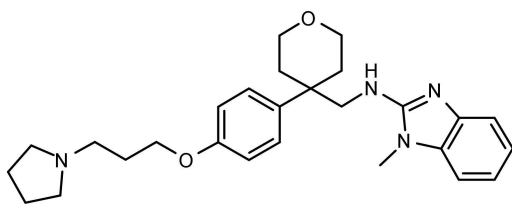
7



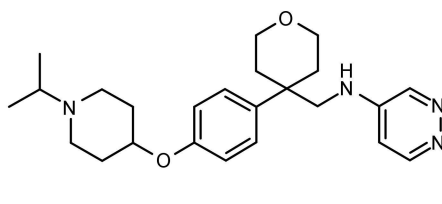
8



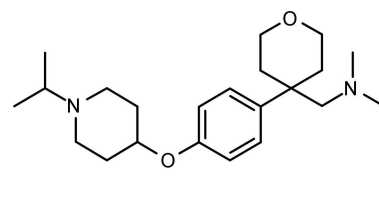
9



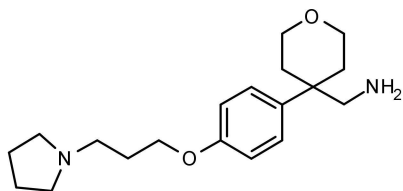
10



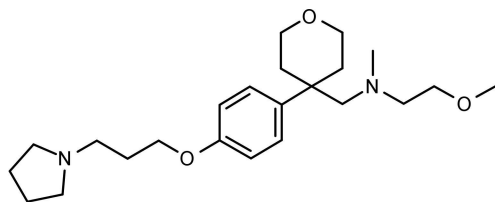
11



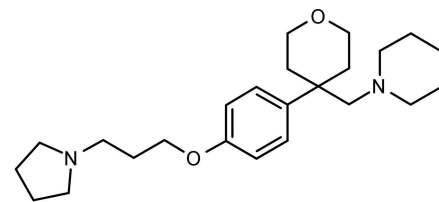
12



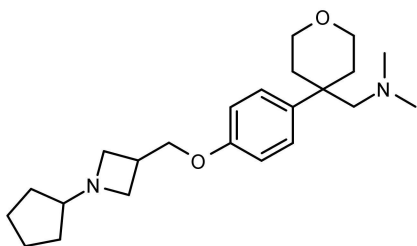
13



14



15



16

Figure 2

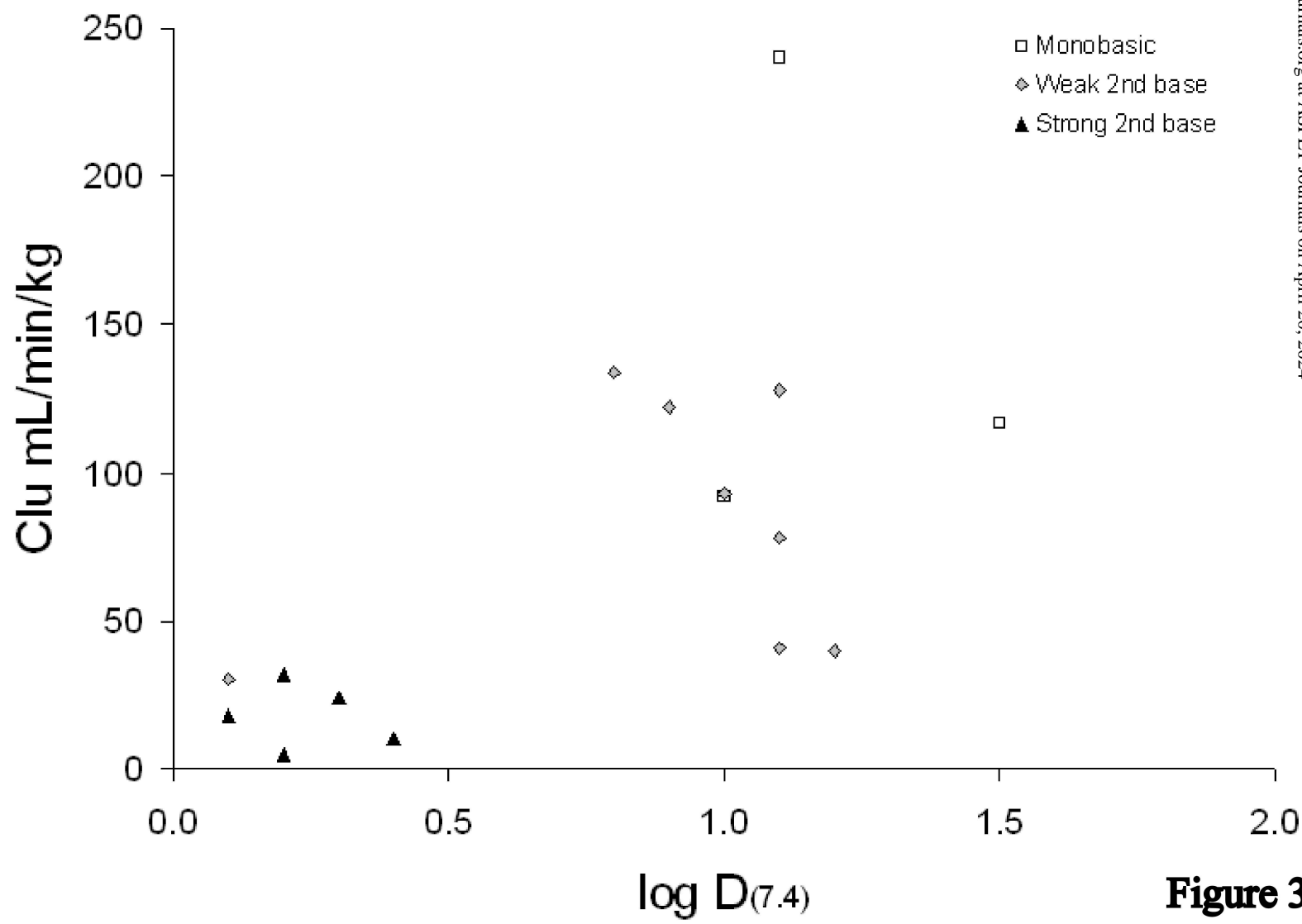


Figure 3

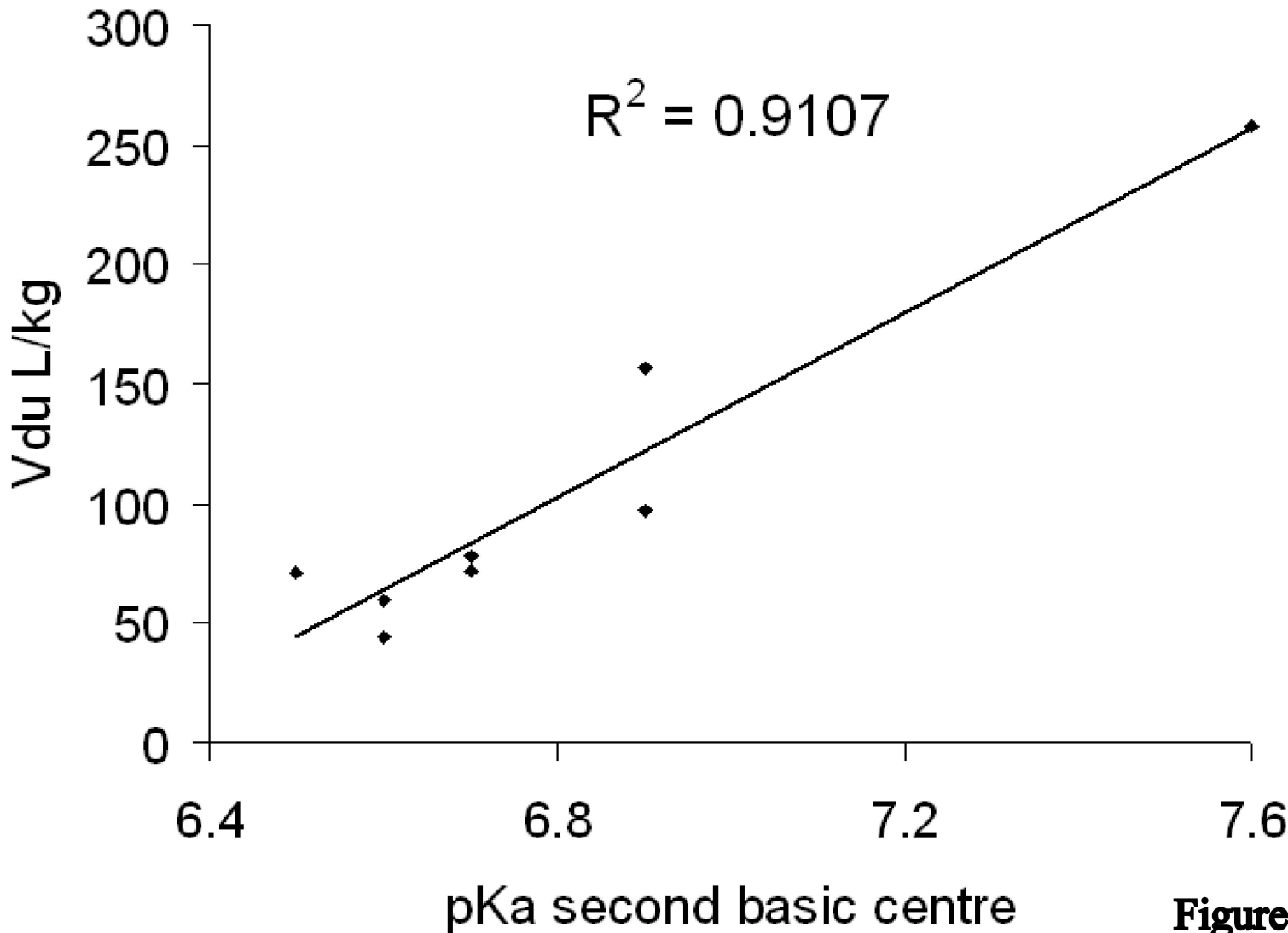


Figure 4

pKa	% ionised at pH 7.4	% ionised at pH 6.4	% ionised at pH 4.4
5.4	1	10	90
6.4	10	50	99
7.4	50	90	99.9
8.4	90	99	99.99
9.4	99	99.9	99.999
10.4	99.9	99.99	99.9999

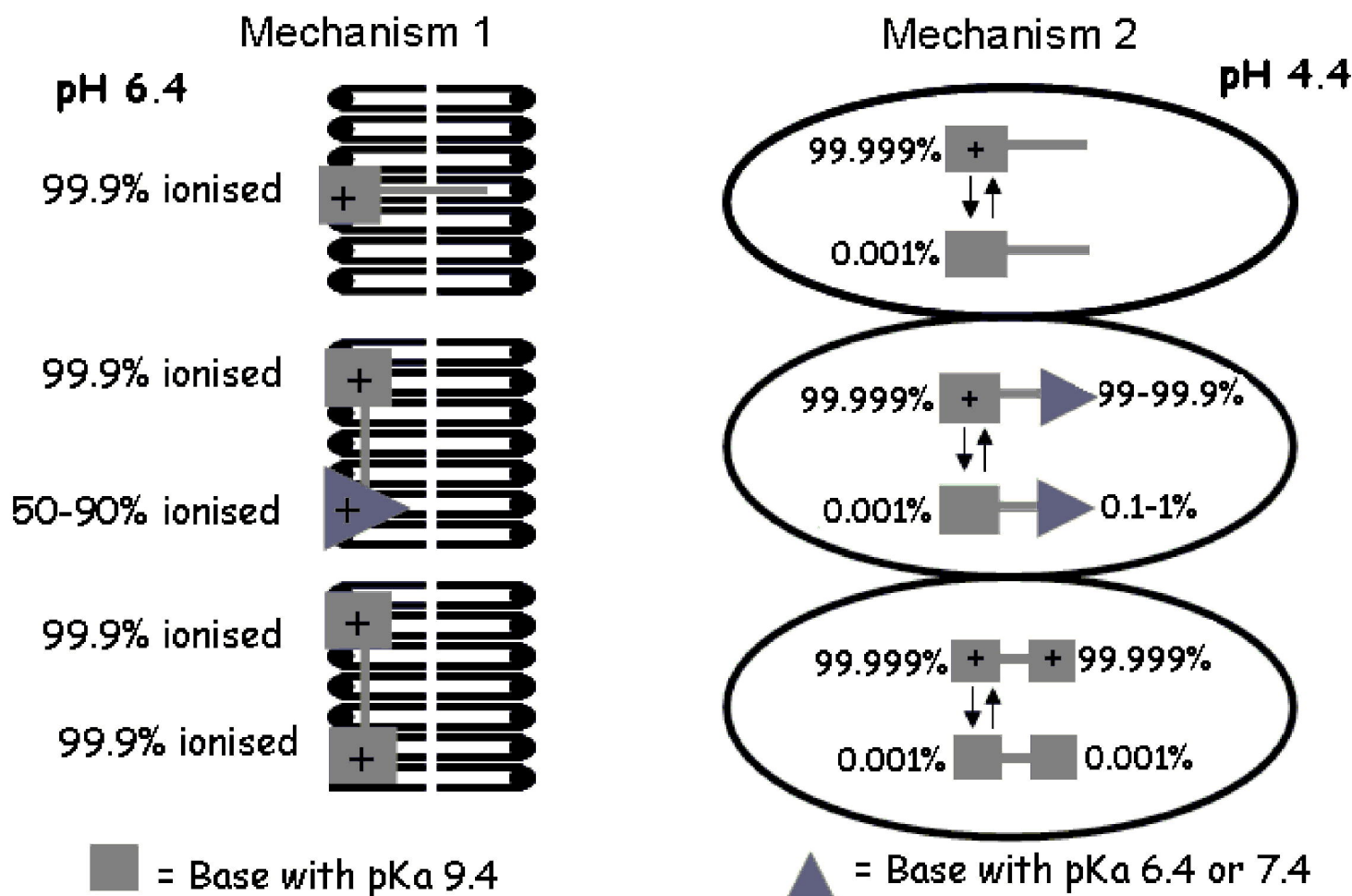


Figure 5